SYNTHESIS AND CHARACTERIZATION OF GRAPHENE FILMS TO BE USED AS TRANSPARENT ELECTRODE IN SOLAR CELLS

Summary

This study explores graphene as a potential transparent conductive electrode (TCE) for silicon heterojunction (SHJ) solar cells instead of tin indium oxide (ITO). Graphene films between 1 and 6 cm^2 were synthesized by chemical vapor deposition and transferred using a polymer-free wet solution method. Raman spectroscopy, scanning electron microscopy (SEM), and atomic force microscopy (AFM) confirmed the good successful transfer of high-quality graphene, with low roughness and minimal defects. Electrical properties were evaluated by Van der Pauw method and Transfer length method, showing a sheet resistance of 89 Ω/sq for graphene, close to that of ITO (58 Ω/sq). These results suggest that graphene offers a viable alternative to ITO for TCE applications in SHJ solar cells.

Keywords: graphene, solar cells, transparent conductive electrode.

1. Introduction

A crucial component in silicon heterojunction (SHJ) solar cells is its transparent conductive electrode (TCE), which must allow sunlight to pass through to the cell surface and collect charge carriers to direct them to the electrical contacts at the same time. Thus, a good TCE must have high transparency and low electrical resistance. Indium tin oxide (ITO) is currently used for this purpose because of its high transmittance, above 80% and low sheet resistance, below 100 Ω/sq (Gageot et al., 2023). However, according to Cui (2023), this is a scarce material, impeding mass production and increasing production costs. In the search for an alternative material to be used as TCE, graphene has emerged as a promising option, being a material with relatively low cost of production and striking structural, optical, and electrical properties (Mandal et al., 2021). Due to this high potential, we grow graphene layers with sizes between 1 and 6 cm^2 and study their structural and electrical properties as TCE on a SHJ cell.

2. Methodology

Graphene is synthesized by chemical vapor deposition (CVD) using copper as a substrate in an H_2 environment, with CH_4 as principal precursor. After this process, we transfer it onto the desired substrate using a polymer-free wet solution method. The substrates were a n-dopped silicon wafer with 285 nm of silicon oxide on top, to evaluate the quality of the synthesized graphene, and an incomplete SHJ cell (of 2.5x2.5 cm^2), in which graphene was deposited in the front surface field (FSF) as shown in Figure 1b. Figure 1 shows a simple scheme of the structure of the SHJ solar cell used in this work.

Graphene
n^+ a-Si:H
i-a-Si:H
c-Si (n)
i-a-Si:H
p^+ a-Si:H
ITO

Fig. 1: Scheme of the SHJ solar cell used in this work with graphene on top.

To evaluate graphene structural properties we performed Raman spectroscopy, scanning electron microscopy (SEM) and atomic force microscopy (AFM). The sheet resistance of graphene and ITO films is measured using Van der Pauw method with the configuration shown in Figure 2a. To assess the contact resistance between the graphene films and silver contacts on top we use the transfer length method (TLM). The geometry of the

© 2026. The Authors. Published by International Solar Energy Society
Selection and/or peer review under responsibility of Scientific Committee
Available at http://proceedings.ises.org

contacts is shown in Figure 2b. A linear fit of a plot of the electrical resistance as a function of the contact spacing allows us to extract those resistances.

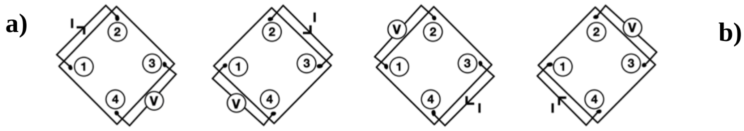

Fig. 2: a) Setup for Van der Pauw method; b) Array of contacts used in this work for TLM: width of silver contacts is 1.05 mm; spacings between contacts are 2.91, 1.92, 1.42, 1.19, 0.94, 0.70 and 0.45 mm.

3. Results and discussion

Figure 3a shows the graphene film floating on H_2O during the transfer process; the area of the film is approximately 6 cm^2. Figure 3b is an edition of Figure 3a for better contrast. Once graphene is floating on water, we transfer it to the desired substrate. The standard substrate is SiO_2, because it enables visual contrast and a structural assessment of the nanomaterial.

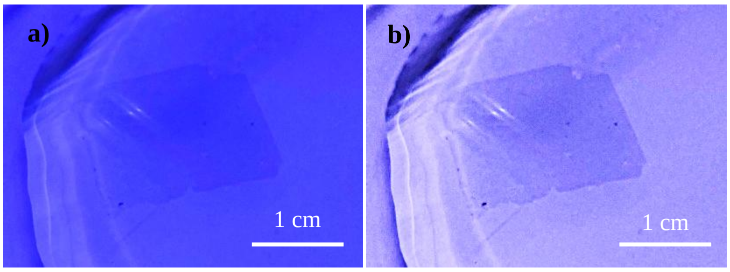

Fig. 3: a) Graphene film floating on H2O during the transfer process; b) Edition of Figure 3a for better contrast.

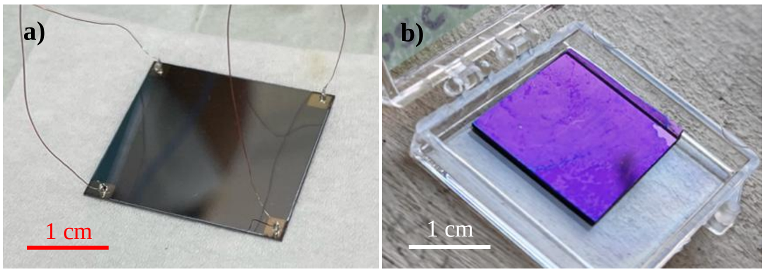

Fig. 4: a) SHJ solar cell with graphene on top and electrical contacts for Van der Pauw method; b) Graphene film on SiO_2.

The intensity ratio of the 2D (2700 cm^{-1}) and G (1580 cm^{-1}) bands in Raman spectrum of the graphene film on SiO_2 allows us to estimate the number of layers in the sample. Figure 5 shows Raman spectrum of two different samples. In Figure 5a can be observed that 2D/G<1, so it corresponds to a three layers graphene sample. Additionally, the D band (1350 cm^{-1}) indicates that the sample has defects, which can be due to islands of the nanomaterial stacked in three layers. In Figure 5b, the 2D/G~2 ratio indicates monolayer graphene, while the subtle D band indicate a low presence of defects.

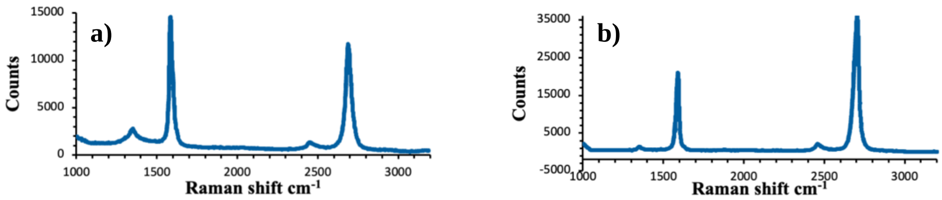

Fig. 5: Raman spectrum of: a) a few-layer graphene sample; b) a monolayer graphene sample.

Figure 4a shows the SHJ cell with the graphene layer on top with the electrical contacts to Van der Pauw measurement. In Figure 4b graphene is on SiO_2, this substrate allows us to observe the nanomaterial due to the visual contrast. As shown in Figure 6, the characteristic peaks of graphene can also be observed in the Raman spectrum of the graphene film on the front surface field (n^+ a-Si:H layer) of the SHJ solar cell. This confirms the transfer of a high-quality graphene film onto the solar cell.

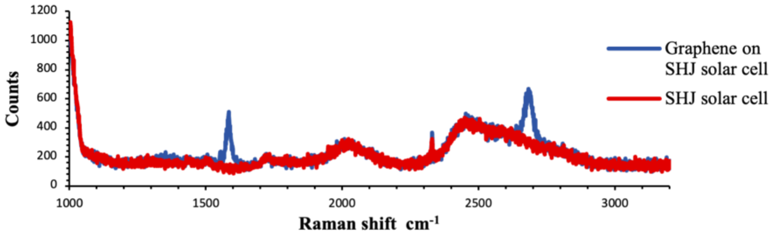

Fig. 6: Raman spectrum of the n-side SHJ solar cell with and without graphene.

Figure 7a shows a SEM image of graphene on SiO_2, which shows that a full coverage of the substrate is achieved. An AFM image of the graphene surface on the SHJ solar cell (Figure 7) confirms that the sample doesn't have fissures on a scale of 12.97 μm^2. However, it has small wrinkles typical of the transfer method. The average roughness of the sample is 12.5 nm.

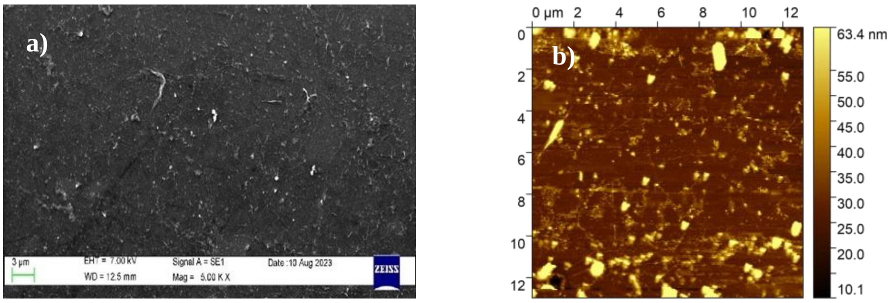

Fig. 7: a) SEM image of graphene on SiO_2; b) AFM image of graphene surface on the n-side SHJ solar cell.

Finally, the results for the graphene sheet resistance show that the nanomaterial on n-side SHJ solar cell are in the order of 89 Ω/sq, which is comparable to the ITO film, which showed a sheet resistance of 58 Ω/sq.

4. Conclusions

We successfully covered the surface of SHJ solar cells with graphene over an approximate area of 6 cm^2, which is a considerable size for a graphene sample. The graphene sheet resistance measurement is very similar to that of ITO, confirming that this material can be a good alternative to be used as TCE in solar cells. Although the resistance value obtained was slightly higher than ITO, it remains within a range suitable for photovoltaic applications.

In addition to its electrical performance, graphene offers other advantages over ITO, such as mechanical flexibility, chemical stability, and the possibility of lower-cost and scalable production. These characteristics make it an interesting alternative for applications in flexible optoelectronic devices. As the next step, it is necessary to evaluate the photovoltaic performance of the SHJ solar cells covered with graphene, comparing its parameters with those obtained using ITO electrodes. These measurements will allow us to assess the real impact of graphene as a TCE in solar cells, beyond its isolated electrical properties.

5. References

Cui, W., Chen, F., Li, Y., Su, X., and Sun, B. (2023) Status and perspectives of transparent conductive oxide films for silicon heterojunction solar cells. Mater. Today Nano, 22, 100329.

Gageot, T., Veirman, J., Jay, F., Muñoz-Rojas, D., Denis, C., Couderc, R., Ozanne, A.S., Monna, R., Zogbo, S., and Cabal, R. (2023) Feasibility test of drastic indium cut down in SHJ solar cells and modules using ultra-thin ITO layers. Sol. Energy Mater. Sol. Cells, 261.

Mandal, P., Debbarma, J., and Saha, M. (2021) A Review on the Emergence of Graphene in Photovoltaics Industry. Biointerface Res. Appl. Chem., 11 (6), 15009–15036.